

УДК 530.145+539.126

$SU(2) \times SU(2)$ NONLOCAL QUARK MODEL WITH CONFINEMENT AND PION RADIUS

*A. E. Radzhabov*¹, *M. K. Volkov*²

Joint Institute for Nuclear Research, Dubna

The nonlocal version of the $SU(2) \times SU(2)$ symmetric four-quark interaction of the NJL type is considered. Each of the quark lines contains the form factors. These form factors remove the ultraviolet divergences in quark loops and ensure the absence of the poles in the quark propagator (quark confinement). The constituent quark mass $m(0)$ is expressed through the cut-off parameter Λ , $m(0) = \Lambda = 340$ MeV in the chiral limit. These parameters are fixed by the experimental value of the weak pion decay and allow us to describe the mass of the light scalar meson, strong $\rho \rightarrow \pi\pi$ decay and D/S ratio in the decay $a_1 \rightarrow \rho\pi$ in satisfactory agreement with experimental data. The electromagnetic radius of a charged pion and the form factor for the process $\gamma^* \pi^+ \pi^-$ in the region $-1 < q^2 < 1.6$ GeV² are calculated.

Рассматривается нелокальная версия $SU(2) \times SU(2)$ симметричного четырехкваркового взаимодействия NJL-типа. Каждая кварковая линия содержит формфакторы, которые устраняют ультрафиолетовые расходимости кварковых петель и обеспечивают отсутствие полюсов в кварковом пропагаторе (кварковый конфайнмент). Масса конститuentного кварка $m(0)$ выражается через параметр обрезания Λ , $m(0) = \Lambda = 340$ МэВ в киральном пределе. Эти параметры фиксируются экспериментальным значением слабого пионного распада и позволяют описывать массу легкого скалярного мезона, сильный распад $\rho \rightarrow \pi\pi$ и соотношение D/S в распаде $a_1 \rightarrow \rho\pi$ в удовлетворительном согласии с экспериментальными данными. Вычисляются электромагнитный радиус заряженного пиона и формфактор процесса $\gamma^* \rightarrow \pi^+ \pi^-$ в области $-1 < q^2 < 1,6$ ГэВ².

The effective meson Lagrangians obtained on the basis of the local four-quark interaction of the Nambu–Jona-Lasinio (NJL) type satisfactorily describe low-energy meson physics [1,2]. However, these models contain ultraviolet (UV) divergences and do not describe quark confinement. Satisfactory results in these models can be obtained only for light mesons and interactions at low energies in the range of 1 GeV. In order to overcome these restrictions, it is necessary to consider nonlocal versions of these models which allow one to remove UV divergences and describe the quark confinement.

A lot of models of this type were proposed in the last few years. Unfortunately, we cannot give here the full list of references concerning this activity. Therefore, we will concentrate only on the direction connected with the nonlocal quark interaction motivated by the instanton theories [3,4]. Recently, a few nonlocal models of this type were proposed [5–7]. In these models the nonlocal kernel is taken in the separable form where each quark line contains form factor following from instanton theories. These form factors naturally remove UV divergences in quark loops.

¹E-mail: aradzh@thsun1.jinr.ru

²E-mail: volkov@thsun1.jinr.ru

Our model is based on the $SU(2) \times SU(2)$ symmetric action

$$\mathcal{S}(\bar{q}, q) = \int d^4x \left\{ \bar{q}(x) i \hat{\partial}_x q(x) + \frac{G_1}{2} (J_\pi^a(x) J_\pi^a(x) + J_\sigma(x) J_\sigma(x)) - \frac{G_2}{2} (J_\rho^{\mu a}(x) J_\rho^{\mu a}(x) + J_{a_1}^{\mu a}(x) J_{a_1}^{\mu a}(x)) \right\}, \quad (1)$$

where $\bar{q}(x) = (\bar{u}(x), \bar{d}(x))$ are the u and d quark fields. The nonlocal quark currents $J_I(x)$ are expressed as

$$J_I(x) = \int d^4x_1 d^4x_2 f(x_1) f(x_2) \bar{q}(x - x_1) \Gamma_I q(x + x_2), \quad (2)$$

where $f(x)$ is a form factor. The matrices Γ_I are defined as

$$\Gamma_\sigma = \mathbf{1}, \quad \Gamma_\pi^a = i\gamma^5 \tau^a, \quad \Gamma_\rho^{\mu a} = \gamma^\mu \tau^a, \quad \Gamma_{a_1}^{\mu a} = \gamma^5 \gamma^\mu \tau^a,$$

where τ^a are the Pauli matrices and γ^μ, γ^5 are the Dirac matrices.

After bosonization the action becomes

$$\begin{aligned} \mathcal{S}(q, \bar{q}, \sigma, \pi, \rho, \omega, A) = & \int d^4x \left\{ -\frac{\pi^a(x)^2 + \tilde{\sigma}(x)^2}{2G_1} + \frac{(\rho^{\mu a}(x))^2 + (a_1^{\mu a}(x))^2}{2G_2} + \right. \\ & + \bar{q}(x) (i \hat{\partial}_x - eQ \hat{A}(x)) q(x) + \int d^4x_1 d^4x_2 f(x - x_1) f(x_2 - x) \bar{q}(x_1) E(x_1, x) \times \\ & \left. \times (\tilde{\sigma}(x) + \pi^a(x) i \gamma^5 \tau^a + \rho^{\mu a}(x) \gamma^\mu \tau^a + a_1^{\mu a}(x) \gamma^5 \gamma^\mu \tau^a) E(x, x_2) q(x_2) \right\}, \quad (3) \end{aligned}$$

$$E(x, y) = P \exp \left(-ieQ \int_x^y A^\mu(z) dz_\mu \right),$$

where $\tilde{\sigma}, \pi, \rho, a$ are the σ, π, ρ, a_1 meson fields, respectively. Here we introduce photon field A^μ by using the Schwinger phase factor $E(x, y)$. Apart from the usual local quark–photon vertex in the action (3) there appear quark–photon and quark–photon–meson nonlocal vertices generated by $P \exp$. The field $\tilde{\sigma}$ has a nonzero vacuum expectation value $\langle \tilde{\sigma} \rangle_0 = \sigma_0 \neq 0$. In order to obtain a physical scalar field with zero vacuum expectation value, it is necessary to shift the scalar field as $\tilde{\sigma} = \sigma + \sigma_0$. This leads to the appearance of the quark mass function $m(p) = -\sigma_0 f^2(p)$. From the action, Eq. (3), by using $\langle \delta S / \delta \sigma \rangle_0 = 0$, one can obtain the gap equation for the dynamical quark mass

$$m(p) = G_1 \frac{8N_c}{(2\pi)^4} f^2(p) \int d_E^4k f^2(k) \frac{m(k)}{k^2 + m^2(k)}. \quad (4)$$

In order to provide quark confinement we propose an ansatz given by the equation

$$\frac{m^2(p)}{m^2(p) + p^2} = \exp(-p^2/\Lambda^2). \quad (5)$$

It is worth noticing, the form of the left-hand side of Eq. (5) coincides with the integrand in the gap Eq. (4). From Eq. (5) we obtain the following solution:

$$m(p) = \left(\frac{p^2}{\exp(p^2/\Lambda^2) - 1} \right)^{1/2}; \quad (6)$$

here we have only one free parameter Λ ; $m(p)$ does not have any singularities in the whole real axis and exponentially drops as $p^2 \rightarrow \infty$ in the Euclidean domain. From Eq. (4) it follows that the form factors have a similar behavior that provides the absence of UV divergences in our model. At $p^2 = 0$, the mass function is equal to the cut-off parameter Λ , $m(0) = \Lambda$. The pole part of the quark propagator also does not contain singularities that provide quark confinement

$$\frac{1}{m^2(p) + p^2} = \frac{1 - \exp(-p^2/\Lambda^2)}{p^2}. \quad (7)$$

Let us consider the scalar and pseudoscalar mesons. The meson propagators are given by

$$D_{\sigma,\pi}(p^2) = \frac{1}{-G_1^{-1} + \Pi_{\sigma,\pi}(p^2)} = \frac{g_{\sigma,\pi}^2(p^2)}{p^2 - M_{\sigma,\pi}^2}, \quad (8)$$

where $M_{\sigma,\pi}$ are the meson masses; $g_{\sigma,\pi}(p^2)$ are the functions describing renormalization of the meson fields, and $\Pi_{\sigma,\pi}(p^2)$ are the polarization operators. The meson masses $M_{\sigma,\pi}$ are found from the position of the pole in the meson propagator $\Pi_{\sigma,\pi}(M_{\sigma,\pi}^2) = G_1^{-1}$ and the constants $g_{\sigma,\pi}(M_{\sigma,\pi}^2)$ are given by

$$g_{\sigma,\pi}^{-2}(M_{\sigma,\pi}^2) = \left. \frac{d\Pi_{\sigma,\pi}(p^2)}{dp^2} \right|_{p^2=M_{\sigma,\pi}^2}. \quad (9)$$

The pion constant is independent of parameter Λ and takes the form

$$g_\pi^{-2}(0) = \frac{N_c}{4\pi^2} \left(\frac{3}{8} + \frac{\zeta(3)}{2} \right), \quad g_\pi(0) \approx 3.7, \quad (10)$$

here ζ is the Riemann zeta function.

The gap equation and quark condensate take the forms

$$G_1 \Lambda^2 = \frac{2\pi^2}{N_c}, \quad \langle \bar{q}q \rangle_0 = -\frac{N_c}{4\pi^2} \int_0^\infty du u \frac{m(u)}{u + m^2(u)}. \quad (11)$$

The Goldberger–Treiman relation is fulfilled in the model of this kind [4–6]

$$F_\pi = \frac{m(0)}{g_\pi}. \quad (12)$$

From Eq. (12) the value $\Lambda = m(0) = 340$ MeV is obtained for $F_\pi = 93$ MeV. Then, from Eq. (11) we obtain $G_1 = 56.6$ GeV⁻², $\langle \bar{q}q \rangle_0 = -(190$ MeV)³.

We get for sigma meson $M_\sigma = 420$ MeV and $g_\sigma(M_\sigma) = 3.85$. The total decay width is $\Gamma_{(\sigma \rightarrow \pi\pi)} = 150$ MeV. Comparing these results with experimental data, one finds that M_σ is in satisfactory agreement with experiment; however, the decay width is very small. This situation can be explained by the fact that for a correct description of the scalar meson it is necessary to take into account the mixing with the four-quark state [9] and the scalar glueball [10]. Moreover, it has recently been shown that the $1/N_c$ corrections in this channel are rather large [11].

Similarly we can describe the vector and axial-vector mesons. The constants G_2 are fixed by ρ -meson mass and numerically are equal to $G_2 = 6.5$ GeV⁻². Then the a_1 -meson mass is equal to 970 MeV.

The amplitude for the process $\rho \rightarrow \pi\pi$ is $A_{(\rho \rightarrow \pi\pi)}^\mu = g_{(\rho \rightarrow \pi\pi)}(q_1 - q_2)^\mu$, where q_i are momenta of the pions. We obtain $g_{(\rho \rightarrow \pi\pi)} = 5.7$ and the decay width $\Gamma_{(\rho \rightarrow \pi\pi)} = 135$ MeV which is in qualitative agreement with the experimental value 149.2 ± 0.7 MeV [8].

The amplitude for the process $a_1 \rightarrow \rho\pi$ is $A_{(a_1 \rightarrow \rho\pi)}^{\mu\nu} = a_{(a_1 \rightarrow \rho\pi)}g^{\mu\nu} + b_{(a_1 \rightarrow \rho\pi)}p^\nu q^\mu$, where p, q are momenta of a_1, ρ mesons, respectively. We obtain $a_{(a_1 \rightarrow \rho\pi)} = 2.68$ GeV, $b_{(a_1 \rightarrow \rho\pi)} = 16.71$ GeV⁻¹. Amplitude of the decay $a_1 \rightarrow \rho\pi$ contains D and S waves. The ratio of these waves has the form (see [5]):

$$\begin{aligned} D/S &= -\sqrt{2} \frac{(E_\rho - M_\rho)a_{(a_1 \rightarrow \rho\pi)} + b_{(a_1 \rightarrow \rho\pi)}M_{a_1}|\mathbf{q}|^2}{(E_\rho + 2M_\rho)a_{(a_1 \rightarrow \rho\pi)} + b_{(a_1 \rightarrow \rho\pi)}M_{a_1}|\mathbf{q}|^2} = -0.06, \\ |\mathbf{q}|^2 &= \lambda(M_{a_1}^2, M_\rho^2, M_\pi^2)/(2M_{a_1})^2, \quad E_\rho^2 = M_\rho^2 + |\mathbf{q}|^2, \\ \lambda(a, b, c) &= a^2 + b^2 + c^2 - 2ab - 2ac - 2bc. \end{aligned} \quad (13)$$

This ratio is in satisfactory agreement with experimental data $D/S^{\text{exp}} = -0.108 \pm 0.016$. The decay width equals $\Gamma_{(a_1 \rightarrow \rho\pi)} = 90$ MeV. This value is noticeably smaller than the experimental one: 250–600 MeV [8].

In our model, like in all models of this kind, $\pi - a_1$ transitions can be neglected.

The amplitude for the process $\gamma^* \pi^+ \pi^-$ has the form

$$T_{\gamma^* \pi^+ \pi^-} = e(p_+ + p_-)^\mu A^\mu(q) \pi^+(p_+) \pi^-(p_-) F_{\gamma^* \pi^+ \pi^-}(q^2), \quad (14)$$

where $F_{\gamma^* \pi^+ \pi^-}(q^2)$ is pion form factor and $q = p_+ - p_-$. The electromagnetic pion radius $\langle r^2 \rangle_{\text{em}}$ is defined by

$$\langle r^2 \rangle_{\text{em}} = -6 \left. \frac{dF_{\gamma^* \pi^+ \pi^-}(q^2)}{dq^2} \right|_{q^2=0}.$$

In the local NJL model the triangle diagram without ρ meson (Fig. 1, a) gives about 80% of the correct value for the pion radius [12]. Therefore, taking into account the diagram

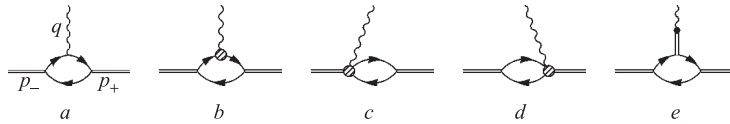


Fig. 1. Diagrams describing charged pion radius: a) the local contribution; b–d) nonlocal contributions; e) the diagrams with the ρ meson

with intermediate ρ meson [12] (Fig. 1, *e*) leads to a too large value for the pion radius in comparison with the experimental value [8]. Indeed, in the local NJL model one has

$$\begin{aligned} \langle r^2 \rangle_{\text{cont}}^{\text{NJL}} &= \frac{N_c}{4\pi^2 f_\pi^2} = 0.342 \text{ fm}^2, & \langle r^2 \rangle_\rho^{\text{NJL}} &= 6/M_\rho^2 = 0.394 \text{ fm}^2, \\ \langle r^2 \rangle_{\text{em}}^{\text{NJL}} &= 0.736 \text{ fm}^2, & & \\ \langle r^2 \rangle_{\text{exp}} &= 0.451 \pm 0.011 \text{ fm}^2. & & \end{aligned} \quad (15)$$

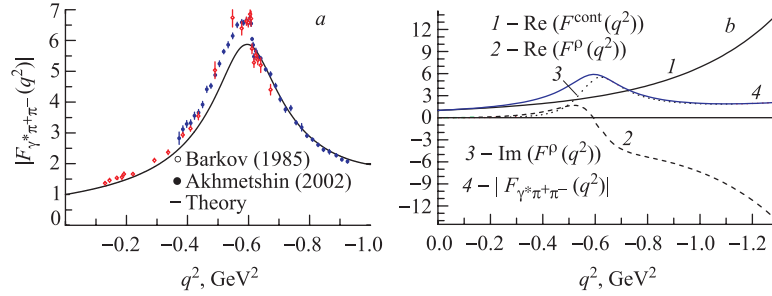


Fig. 2. *a*) The absolute value of charged pion form factor in the time-like region. The finite width of ρ meson is $\Gamma_\rho = 135$ MeV [7]. Experimental data are taken from [13]. *b*) Partial contributions to the charged pion form factor in the time-like region from the contact and ρ -meson diagrams and the absolute value of the charged pion form factor ($\text{Im}(F^{\text{cont}}(q^2)) = 0$)

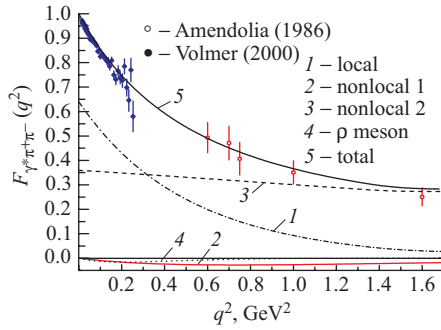


Fig. 3. The charged pion form factor in the space-like region. Partial contributions from diagrams of Fig. 1, *a* (local), Fig. 1, *b* (nonlocal 1), Fig. 1, *c, d* (nonlocal 2), and Fig. 1, *e* (ρ meson) are shown. Experimental data are taken from [14]

smaller than in the NJL model. The latter suppression is due to strong q^2 dependence of the amplitude occurring in the nonlocal model. As a result, we obtain almost one order decrease

Now we show that in contrast, in the nonlocal model, the diagram with the intermediate vector-meson is noticeably suppressed. In the model considered, the contributions to the e.m. pion radius from diagrams in Fig. 1, *a-d* and from diagram in Fig. 1, *e* equal $\langle r^2 \rangle_{\text{cont}} = 0.340 \text{ fm}^2$ and $\langle r^2 \rangle_\rho = 0.047 \text{ fm}^2$, respectively. Then the e.m. pion radius becomes $\langle r^2 \rangle_{\text{em}} = 0.387 \text{ fm}^2$, that is in much better agreement with experimental value than the result of the local model.

Let us consider in more detail the contribution of the ρ -meson diagrams in both the local NJL model and the nonlocal model. These diagrams consist of three parts: the photon- ρ -meson transition, the ρ -meson propagator, and the part describing the $\rho \rightarrow \pi\pi$ vertex. Our calculations show that in the nonlocal quark models the first part is more than twice smaller than in NJL, the second part does not change, and the third part is four times smaller than in the NJL model. The latter suppression is due to strong q^2 dependence of the amplitude occurring in the nonlocal model. As a result, we obtain almost one order decrease

of the ρ -meson diagram contribution in the nonlocal model with respect to the prediction of the local NJL model.

The charged pion form factors $F_{\gamma^* \pi^+ \pi^-}(q^2)$ in the time-like and space-like regions are shown in Figs. 2, 3.

The vector-meson diagrams play a very important role in the description of the pion form factor $F_{\gamma^* \pi^+ \pi^-}$ in the time-like region. These diagrams allow one not only to describe the ρ -meson resonance but also to obtain a correct behavior of the form factor in the region $-q^2 > M_\rho^2$. It should be noted that the contact and vector meson diagrams increase in absolute values in the region $-q^2 > M_\rho^2$, but they have opposite signs. As a result, the total contribution decreases (see Fig. 2) in agreement with experimental tendency [13].

Acknowledgements. The authors thank A. E. Dorokhov for fruitful collaboration. The work is supported by RFBR Grant No. 02-02-16194 and the Heisenberg–Landau program.

REFERENCES

1. Ebert D., Volkov M. K. // *Z. Phys. C*. 1983. V. 16. P. 205;
Volkov M. K. // *Ann. Phys.* 1984. V. 157. P. 282;
Volkov M. K. // *Sov. J. Part. Nucl.* 1986. V. 17. P. 186;
Ebert D., Reinhardt H. // *Nucl. Phys. B*. 1986. V. 271. P. 188;
Ebert D., Reinhardt H., Volkov M. K. // *Prog. Part. Nucl. Phys.* 1994. V. 33. P. 1.
2. Vogl U., Weise W. // *Prog. Part. Nucl. Phys.* 1991. V. 27. P. 195;
Klevansky S. P. // *Rev. Mod. Phys.* 1992. V. 64. P. 649.
3. Shuryak E. V. // *Nucl. Phys. B*. 1982. V. 203. P. 93;
Diakonov D., Petrov V. Y. // *Nucl. Phys. B*. 1984. V. 245. P. 259; 1986. V. 272. P. 457.
4. Dorokhov A. E., Tomio L. // *Phys. Rev. D*. 2000. V. 62. P. 014016;
Anikin I. V., Dorokhov A. E., Tomio L. // *Part. Nucl.* 2000. V. 31. P. 509.
5. Bowler R. D., Birse M. C. // *Nucl. Phys. A*. 1995. V. 582. P. 655;
Plant R. S., Birse M. C. // *Nucl. Phys. A*. 1998. V. 628. P. 607.
6. Dorokhov A. E., Broniowski W. // *Phys. Rev. D*. 2002. V. 65. P. 094007;
Dorokhov A. E., Radzhabov A. E., Volkov M. K. JINR, E2-2003-51. Dubna, 2003; *Phys. At. Nucl.* 2004. V. 67 (to be published).
7. Radzhabov A. E., Volkov M. K. hep-ph/0305272; *Eur. Phys. J. A* (to be published);
Dorokhov A. E., Radzhabov A. E., Volkov M. K. hep-ph/0311359; *Eur. Phys. J. A* (submitted).
8. Hagiwara K. et al. (*Particle Data Group Collab.*) // *Phys. Rev. D*. 2002. V. 66. P. 010001.
9. Jaffe R. L. // *Phys. Rev. D*. 1977. V. 15. P. 267–281.
10. Volkov M. K., Yudichev V. L. // *Eur. Phys. J. A*. 2001. V. 10. P. 109.
11. Plant R. S., Birse M. C. // *Nucl. Phys. A*. 2002. V. 703. P. 717.
12. Volkov M. K. // *Phys. At. Nucl.* 1997. V. 60. P. 997.

13. *Barkov L. M. et al. // Nucl. Phys. B. 1985. V. 256. P. 365;*
Akhmetshin R. R. et al. (CMD-2 Collab.) // Phys. Lett. B. 2002. V. 527. P. 161;
Akhmetshin R. R. et al. (CMD-2 Collab.). Reanalysis of hadronic cross-section measurements at
CMD-2. hep-ex/0308008.
14. *Amendolia S. R. et al. (NA7 Collab.) // Nucl. Phys. B. 1986. V. 277. P. 168;*
Volmer J. et al. (The Jefferson Lab F(pi) Collab.) // Phys. Rev. Lett. 2001. V. 86. P. 1713.